INSTITUTE FOR HIGH ENERGY PHYSICS

High statistic study of the $K^- \to \pi^0\mu^-\nu$ decay

O.P. Yushchenko, S.A. Akimenko, K.S. Belous, G.I. Britvich, I.G.Britvich, K.V.Datsko, A.P. Filin, A.V. Inyakin, A.S. Konstantinov, V.F. Konstantinov, I.Y. Korolkov, V.A. Khmelnikov, V.M. Leontiev, V.P. Novikov, V.F. Obraztsov, V.A. Polyakov, V.I. Romanovsky, V.M. Ronjin, V.I. Shelikhov, N.E. Smirnov, O.G. Tchikilev, V.A.Uvarov.

Institute for High Energy Physics, Protvino, Russia

V.N. Bolotov, S.V. Laptev, A.R. Pastsjak, A.Yu. Polyarush.

Institute for Nuclear Research, Moscow, Russia

Abstract

The decay $K^- \to \pi^0\mu^-\nu$ has been studied using in-flight decays detected with the "ISTRA+" spectrometer. About 540K events were collected for the analysis. The λ_+ and λ_0 slope parameters of the decay form-factors $f_+(t)$, $f_0(t)$ have been measured : $\lambda_+ = 0.0277 \pm 0.0013(\text{stat}) \pm 0.0009(\text{syst})$, $\lambda_0 = 0.0183 \pm 0.0011(\text{stat}) \pm 0.0006(\text{syst})$, and $d\lambda_0/d\lambda_+ = -0.348$. The limits on the possible tensor and scalar couplings have been derived: $f_T/f_+(0) = -0.0007 \pm 0.0071$, $f_S/f_+(0) = 0.0017 \pm 0.0014$. No visible non-linearity in the form-factors have been observed.

1 Introduction

The decay $K \to \mu\nu\pi^0(\mathrm{K}_{\mu 3})$ provides unique information about the dynamics of the strong interactions. It has been a testing ground for such theories as current algebra, PCAC, Chiral Perturbation Theory(ChPT). In this paper we present a high-statistics measurement ($\sim$ 537K events) of the Dalitz plot density in this decay. This study has a particular interest in view of new two-loop order (p^6) calculations for K_{l3} in ChPT [1].

The $\mathrm{K}_{\mu 3}$ decay is also known to be a key one in hunting for phenomena beyond the Standard Model (SM). In particular, significant efforts have been invested into T-violation searches, by the measurements of the muon transverse polarization σ_T [2], as well as into searches for the non-SM contributions into the decay amplitude [3].

In our analysis we present new search for scalar (S) and tensor (T) interactions by fitting the $K_{\mu 3}$ Dalitz plot distribution, similar to the procedure used in the K_{e3} decay studies[4].

2 Experimental setup

The experiment has been performed at the IHEP 70 GeV proton synchrotron U-70. The experimental setup "ISTRA+" (Fig.1) was described in some details in our paper [5].

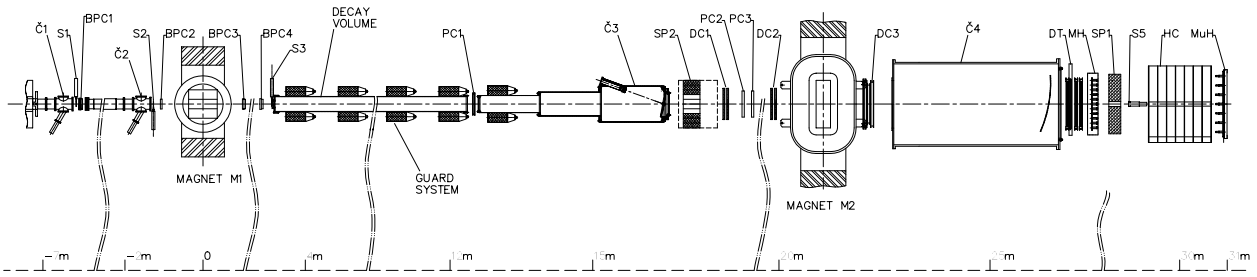

Figure 1: Elevation view of the "ISTRA+" detector.

The setup is located in a negative unseparated secondary beam. The beam momentum is $\sim$ 25 GeV with $\Delta p/p \sim 1.5\%$. The admixture of K^- in the beam is $\sim 3\%$. The beam intensity is $\sim 3 \cdot 10^6$ per 1.9 sec. of the U-70 spill. The beam particles are deflected by the beam magnet M_1 and are measured by $BPC_1 \div BPC_4$ proportional chambers with 1 mm wire spacing. The kaon identification is performed by $\check{C}_0 \div \check{C}_2$ threshold $\check{C}$-counters.

The 9 meter long vacuumed decay volume is surrounded by 8 lead-glass rings $LG_1 \div LG_8$ which are used as the veto system for low energy photons. The photons radiated at large angles are detected by the lead-glass calorimeter SP_2.

The decay products are deflected by the spectrometer magnet M2 with a field integral of 1 Tm. The track measurement is performed by 2-mm-step proportional chambers ($PC_1 \div PC_3$), 1-cm-cell drift chambers ($DC_1 \div DC_3$), and by 2-cm-diameter drift tubes ($DT_1 \div DT_4$). Wide aperture threshold Čerenkov counters ($\check{C}_3$ and $\check{C}_4$) are filled with helium and are not used in these measurements.

The photons are measured by the lead-glass calorimeter SP_1 which consists of 576 counters. The counter transverse size is 5.2×5.2 cm and the length is about 15 X_0.

The scintillator-iron sampling hadron calorimeter HC is subdivided into 7 longitudinal sections 7×7 cells each. The 11×11 cell scintillating hodoscope is used for the improvement of the time resolution of the tracking system. MuH is a 7×7 cell scintillating muon hodoscope.

The trigger is provided by $S_1 \div S_5$ scintillation counters, $\check{C}_0 \div \check{C}_2$ Cerenkov counters, and the analog sum of amplitudes from last dinodes of the SP_1 :

$$T = S_1 \cdot S_2 \cdot S_3 \cdot \bar{S}_4 \cdot \check{C}_0 \cdot \bar{\check{C}}_1 \cdot \bar{\check{C}}_2 \cdot \bar{S}_5 \cdot \Sigma(SP_1),$$

where S_4 is the scintillator counter with a hole to suppress the beam halo, S_5 is the counter located downstream the setup at the beam focus. This part of the trigger is intended to identify beam kaons and to kill undecayed particles. It is designed on purpose, in a very simple way, to avoid any bias. $\Sigma(SP_1)$ requires that the analog sum of amplitudes from the SP_1 be larger than ∼700 MeV - the MIP signal. The last requirement serves to suppress the dominating $K \to \mu\nu$ decay. A part of events (10%) which do not satisfy the $\Sigma(SP_1)$ requirement is also recorded to provide the information for muon identification studies.

3 Events selection

During run in Winter 2001, 332M events were logged on tapes. This statistics is complemented by about 130M MC events generated with Geant3 [6] Monte Carlo program. The MC generation includes a realistic description of the setup with decay volume entrance windows, tracking chambers windows, chambers gas mixtures, sense wires and cathode structures, Čerenkov counters mirrors and gas, the shower generation in EM calorimeters, etc.

The data processing starts with the beam particle reconstruction in $BPC_1 \div BPC_4$. Then secondary tracks are looked for in the decay tracking system and events with one good negatively charged track are selected. The decay vertex is reconstructed by means of the unconstrained vertex fit of the beam and decay tracks.

A clustering procedure is used to find showers in the SP_1 calorimeter, and the two-dimensional pattern of the shower is fitted with the MC-generated patterns to reconstruct its energy and position.

The muon identification is done using the information from electromagnetic and hadronic calorimeters. First of all, the energy deposition in the SP_1 associated with the track (counted in the 3x3 matrix around the track extrapolation to the SP_1) is required to be less than 500 MeV. This cut is intended to suppress the electron tracks. The sum of ADC counts from the HC counters associated with remaining tracks is demanded to be less than 200 (see Figure 2). And, finally, the ratio of the associated ADC signals in the last three layers of HC to the total associated ADC sum to be greater than 0.05 is required (Figure 3 shows this value for the tracks which pass the first two selection criteria).

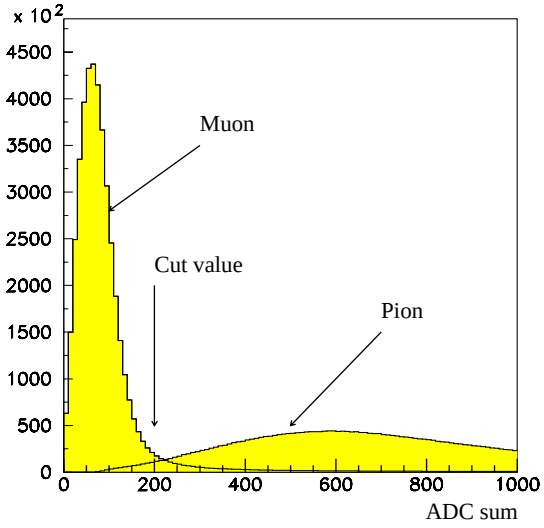

Figure 2: The ADC sum in HC for the track-associated cells.

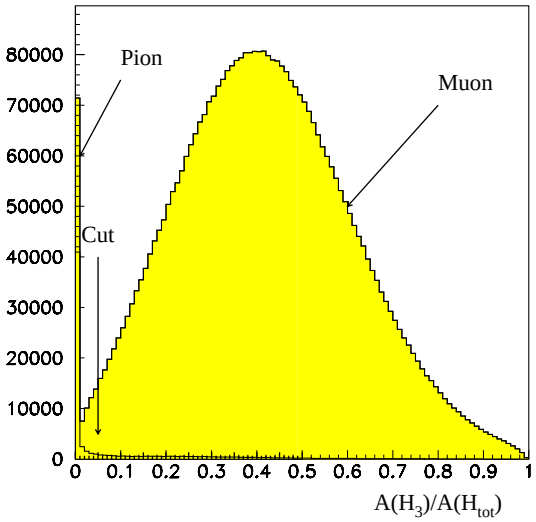

Figure 3: The ratio of the track-associated ADC signals in the last three layers of HC to the total associated signal.

The figures 2 and 3 are obtained with the clean π^- and μ^- samples selected from the real data. The pion data sample is composed from selected $K^- \to \pi^-\pi^0$ decays, and the muon one from the $K^- \to \mu^-\nu_\mu$ decays.

The efficiency of the muon identification and the probability of the $\pi \to \mu$ assignment were found to be 88% and 0.03 respectively.

The events with one charged track identified as muon and two additional showers in the SP_1 are selected for further processing.

The selected events are required to pass 2C $K \to \mu\nu\pi^0$ fit, with a probability of the fit $P_{\rm fit} > 0.005$. The angle between π^0 and μ^- in the kaon rest frame after 2C fit was found to be a good variable for the further background suppression (see Figure 4). The background from the surviving $K^- \to \pi^-\pi^0$ events is concentrated at $\cos\theta \sim -1$, and the selected cut $\cos\theta_{\pi\mu} > -0.95$ removes practically all the background. The missing energy $E_\nu = E_K - E_\mu - E_{\pi^0}$ after the angular cut is shown in Figure 5. The signal Monte-Carlo events for Figures 4 and 5 are weighted with the $K_{\mu 3}$ matrix element where we use $\lambda_+ = 0.0286$ (fixed from our K_{e3} measurements [4]) and $\lambda_0 = 0.017$ (from the ChPT O(p^4) calculations [7]).

We estimate the surviving background contribution to be around 0.3%.

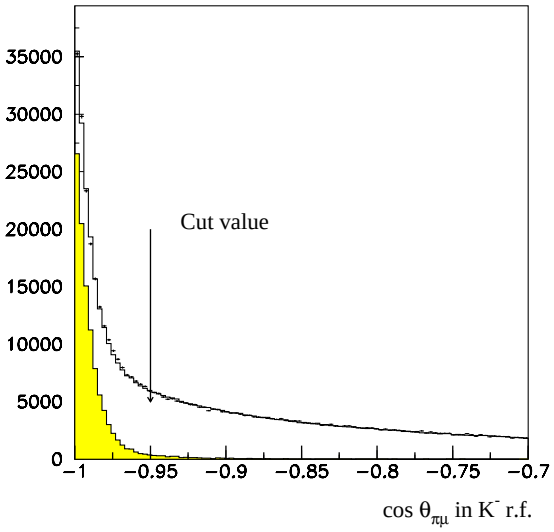

Figure 4: The cosine of the $\pi - \mu$ angle in the kaon rest frame after 2C fit. The points with errors are data and the solid histogram is MC. The shaded area shows the background contribution.

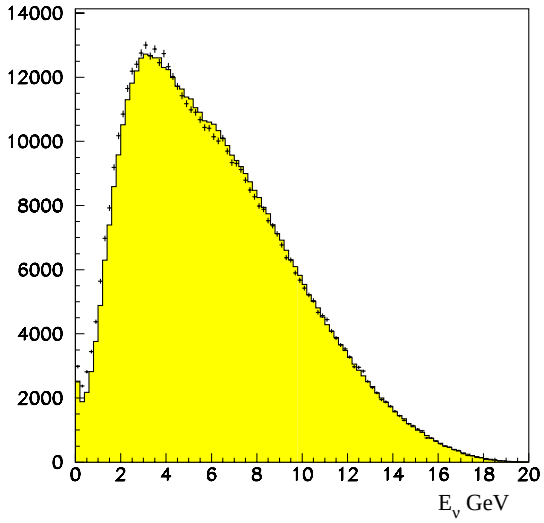

Figure 5: The E_ν compared with MC.

4 Analysis

After the procedure described in the previous section, 537K events are selected in the real data. The distribution of the events over the Dalitz plot is shown in Figure 6.

The most general Lorentz-invariant form of the matrix element for the $K^- \to l^-\nu\pi^0$ decay is [8]:

$$M = \frac{G_F V_{us}}{2}\bar{u}(p_\nu)(1+\gamma^5)[2m_K f_S - [(P_K+P_\pi)_\alpha f_+ + (P_K-P_\pi)_\alpha f_-]\gamma^\alpha + i\frac{2f_T}{m_K}\sigma_{\alpha\beta}P_K^\alpha P_\pi^\beta]v(p_l) \quad (1)$$

It consists of scalar, vector, and tensor terms. The $f_\pm$ form-factors are the functions of $t = (P_K - P_\pi)^2$. In the Standard Model (SM), the W-boson exchange leads to the pure vector term. The scalar and/or tensor terms which are "induced" by EW radiative corrections are negligibly small, i.e nonzero scalar or tensor form-factors would indicate the physics beyond the SM.

The term in the vector part, proportional to f_-, is reduced (using the Dirac equation) to the scalar form-factor. In the same way, the tensor term is reduced to a mixture of the scalar and vector form-factors. The redefined vector (V) and scalar (S) terms, and the corresponding Dalitz plot density in the kaon rest frame ($\rho(E_\pi, E_l)$) are [9]:

$$\rho(E_\pi, E_l) \quad \sim \quad A \cdot |V|^2 + B \cdot Re(V^* S) + C \cdot |S|^2 \quad (2)$$

$$
\begin{aligned}
V &= f_+ + (m_l/m_K) f_T \\
S &= f_S + (m_l/2m_K) f_- + \left(1 + \frac{m_l^2}{2m_K^2} - \frac{2E_l}{m_K} - \frac{E_\pi}{m_K}\right) f_T \\
A &= m_K(2E_l E_\nu - m_K \Delta E_\pi) - m_l^2 (E_\nu - \frac{1}{4}\Delta E_\pi) \\
B &= m_l m_K (2E_\nu - \Delta E_\pi);\ E_\nu = m_K - E_l - E_\pi \\
C &= m_K^2 \Delta E_\pi;\ \Delta E_\pi = E_\pi^{max} - E_\pi;\ E_\pi^{max} = \frac{m_K^2 - m_l^2 + m_\pi^2}{2m_K}
\end{aligned}
$$

Following [7] the scalar form-factor f_0 is introduced:

$$
f_0(t) = f_+(t) + \frac{t}{m_K^2 - m_\pi^2} f_-(t), \tag{3}
$$

and we assume, at most, the quadratic dependence of $f_+,\ f_0$ on t:

$$
f_+(t) = f_+(0)\left(1 + \lambda_+ t/m_\pi^2 + \lambda_+^{'} t^2/m_\pi^4\right), \quad f_0(t) = f_+(0)\left(1 + \lambda_0 t/m_\pi^2 + \lambda_0^{'} t^2/m_\pi^4\right). \tag{4}
$$

Finally, one gets from Eq. (3):

$$
f_- = f_+(0)\frac{m_K^2 - m_\pi^2}{m_\pi^2} \cdot \left(\lambda_0 - \lambda_+ + \frac{t}{m_\pi^4}(\lambda_0^{'} - \lambda_+^{'})\right) \tag{5}
$$

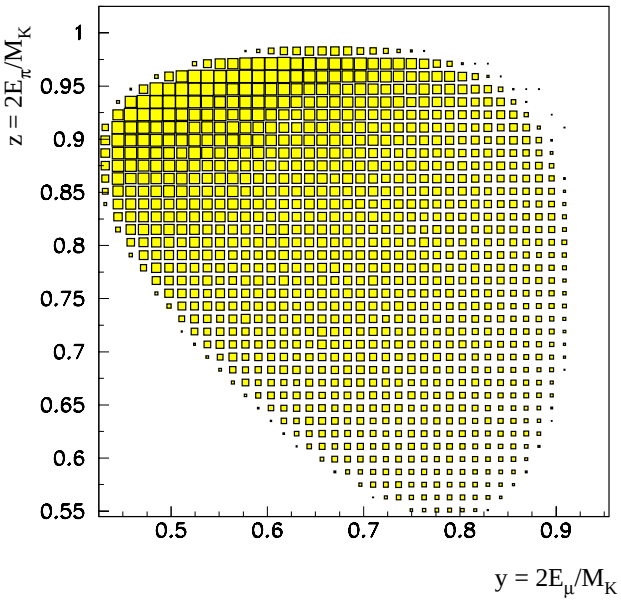

Figure 6: Dalitz plot for the selected $K \to \mu\nu\pi^0$ events after the 2C fit.

The procedure of the extraction of the form-factor parameters starts with the subdivision of the Dalitz plot region $y = 0.425 \div 0.955;\ z = 0.545 \div 1.025$ into 40×40 bins.

The signal MC was generated with the constant matrix element and we have to calculate the amplitude-induced weights during the fit procedure. One can observe that the Dalitz-plot density function $\rho(y, z)$ of (2) can be presented in the factorisable form, i.e

$$\rho(y, z) = \sum_{\alpha=1,18} F_\alpha(\lambda_+, \lambda_+^{'}, \lambda_0, \lambda_0^{'}, f_S, f_T) \cdot K_\alpha(y, z), \tag{6}$$

where F_α are simple bilinear functions of the form-factor parameters and $K_\alpha(y, z)$ are the kinematic functions which are calculated from the MC-truth information. For each α, the sums of $K_\alpha(y, z)$ over events are accumulated in the Dalitz plot bins (i,j) to which the MC events fall after the reconstruction. Finally, every bin in the Dalitz plot gets 18 weights $W_\alpha(i, j)$ and the density function $r(i, j)$ which enters into the fitting procedure is constructed:

$$r(i, j) = \sum_{\alpha=1,18} F_\alpha(\lambda_+, \lambda_+^{'}, \lambda_0, \lambda_0^{'}, f_S, f_T) \cdot W_\alpha(i, j) \tag{7}$$

This method allows one to avoid the systematic errors due to the "migration" of the events over the Dalitz plot due to the finite experimental resolution and automatically takes into account the efficiency of the reconstruction and selection procedures.

To take into account the finite number of MC events in the particular bin and strong variation of the real data events over the Dalitz plot, we minimize a $-\mathcal{L}$ function defined as [10]:

$$-\mathcal{L} = 2\sum_j n_j \ln\left[\frac{n_j}{r_j}\left(1 - \frac{1}{m_j + 1}\right)\right] + 2\sum_j (n_j + m_j + 1) \ln\left(\frac{1 + \frac{r_j}{m_j}}{1 + \frac{n_j}{m_j+1}}\right), \tag{8}$$

where the sum runs over all populated bins, and n_j, r_j and m_j are the number of data events, expected events and generated Monte Carlo events respectively. For large m_j Eq. (8) reduces to the more familiar expression

$$-\mathcal{L} = \sum_j [2(r_j - n_j) + 2n_j \ln n_j/r_j]$$

The minimization is performed by means of the "MINUIT" program [11]. The errors are calculated by "MINOS" procedure of "MINUIT" at the level $\Delta\mathcal{L} = 1$, corresponding to 68% coverage probability for 1 parameter.

5 Results

A fit of the $K_{\mu 3}$ data with $f_S = f_T = \lambda_+^{'} = \lambda_0^{'} = 0$ gives the following result for λ_+ and λ_0: $\lambda_+ = 0.0277 \pm 0.0013$; $\lambda_0 = 0.0183 \pm 0.001$. The $\lambda_+ - \lambda_0$ correlation parameter is found to be $d\lambda_0/d\lambda_+ = -0.348$. The total number of bins is 1054 and $\chi^2/\mathrm{ndf} = 1.008$. The quality of the fit is illustrated in figures 7 and 8 where the projected variables $y = 2E_\mu/m_K$ and $z = 2E_{\pi^0}/m_K$ are presented.

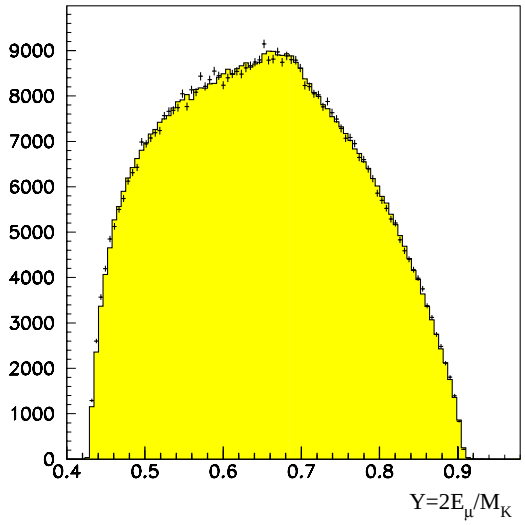

Figure 7: Y distribution.
The points with errors are the real data and the shaded area – signal MC.

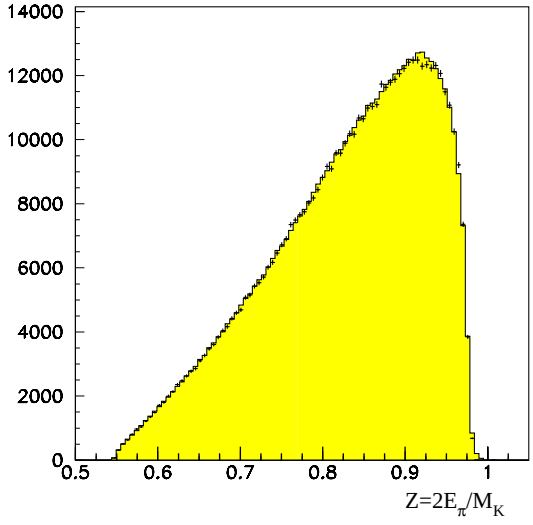

Figure 8: Z distribution.
The points with errors are the real data and the shaded area – signal MC.

The value $\lambda_+^\mu = 0.0277 \pm 0.0013$ is in a good agreement with that extracted from the analysis of our K_{e3} data [4]: $\lambda_+^e = 0.0286 \pm 0.00054(stat) \pm 0.0006(syst)$ (the statistical error ± 0.0008 presented in [4] was obtained with $\Delta\mathcal{L} = 2.3$, corresponding to 68% coverage probability for 2-parameter fit), i.e, our data do not contradict $\mu - e$ universality.

In addition to the fits described above, Table 1 represents the fits with possible nonlinear terms in f_+ and f_0 (Eq. 4) as well as the fits with tensor and scalar contributions (Eq. 1).

Every row of the Table 1 represents a particular fit where the parameters shown without errors are fixed. The second row shows a fit where the nonlinearity is allowed in $f_+(t)$. One can observe $\lambda_+ - \lambda'_+$ correlation that results in the significant λ_+ errors enhancement and visible shift of λ_+ and λ_0 parameters. The fitted value of λ'_+ is compatible with zero, while we can not exclude some nonlinearity. The third row represents a fit with the value of λ'_+ parameter extracted from the analysis of the data on pion scalar form-factors [1]: $\lambda'_+ = 3.2 \cdot m_\pi^4 = 0.001063$. In a similar way λ'_0 parameter is strongly correlated with λ_0 and is compatible with zero (row 4).

We do not see any tensor contribution in our data (row 5). The last row of the Table 1 represents a search for the scalar contribution. As one can see from the Eq. (2), the f_S term is 100% anti-correlated with V-A contribution $(m_\mu/2m_K)f_-$, where $f_- = f_+(0)(\lambda_0 - \lambda_+)\frac{m_K^2 - m_\pi^2}{m_\pi^2}$, i.e an independent estimate of this term is necessary. A possible way consists in fixing λ_0 at the value calculated in the O(p^4) ChPT: $\lambda_0^{\rm th} = 0.017 \pm 0.004$ [7]. The error ± 0.004 in the theoretical prediction induces an additional error of ± 0.0053 in $f_S/f_+(0)$.

λ_+, λ_0	λ'_+, λ'_0	$f_T/f_+(0)$, $f_S/f_+(0)$	Fit prob.
0.0277 ± 0.0013	0.	0.	0.425
0.0183 ± 0.0011	0.	0.	
0.0215 ± 0.0060	0.0010 ± 0.0010	0.	0.451
0.0160 ± 0.0021	0.	0.	
0.0216 ± 0.0013	0.001063	0.	0.451
0.0163 ± 0.0011	0.	0.	
0.0276 ± 0.0014	0.	0.	0.421
0.0170 ± 0.0059	0.0002 ± 0.0008	0.	
0.0276 ± 0.0014	0.	-0.0007 ± 0.0071	0.422
0.0183 ± 0.0011	0.	0.	
0.0277 ± 0.0013	0.	0.	0.421
0.017	0.	0.0017 ± 0.0014	

Table 1. The $K_{\mu 3}$ fits.

Different sources of systematics are investigated. We allow variations of the muon selection cuts, angular cut and 2C-fit probability cut. The Dalitz plot binning, signal and background MC variations are also applied.

The resulting systematic uncertainties are as follows:

- $\Delta\lambda_+ = 0.0009$ and $\Delta\lambda_0 = 0.0006$;
- $\Delta f_T/f_+(0) = 0.002$ and $\Delta f_S/f_+(0) = 0.0009$

6 Summary and conclusions

The $K^-_{\mu 3}$ decay has been studied using in-flight decays of 25 GeV K^- detected by the "ISTRA+" magnetic spectrometer.

The λ_+ parameter of the vector form-factor is measured to be:

$$\lambda_+ = 0.0277 \pm 0.0013\ (stat) \pm 0.0009\ (syst)$$

The λ_0 parameter of the scalar form-factor is defined:

$$\lambda_0 = 0.0183 \pm 0.0011\ (stat) \pm 0.0006\ (syst)$$

The comparison of the λ_+ parameter with that obtained from our K_{e3} data shows $e-\mu$ universality.

It is, at present, the best measurement of these parameters. It is in a reasonable agreement with $O(p^4)$ ChPT prediction as well as with recent λ_0 measurements from the $\Gamma(K_{\mu 3})/\Gamma(K_{e3})$ ratio [12].

Possible quadratic contributions in the vector and scalar form-factors are compatible with zero, further studies are necessary to perform a detailed comparison of our data with $O(p^6)$ ChPT calculations [1].

The limits on possible tensor and scalar couplings are derived from the combined fit:

$$f_T/f_+(0) = -0.0007 \pm 0.0071\ (stat) \pm 0.002\ (syst);$$

$$f_S/f_+(0) = 0.0017 \pm 0.0014\ (stat) \pm 0.0009\ (syst) \pm 0.0053\ (theor)$$

The work is supported by the RFBR grant N03-02-16330.

References

[1] J.Bijnens and P.Talavera, Nucl.Phys. **B669**(2003), 341.

[2] M. Abe et al., Nucl.Phys. **A721**(2003), 445.

[3] I.V.Ajinenko et al., Phys.Atom.Nucl. **66**(2003), 105; Yad.Fiz. **66**(2003), 107.

[4] I.V.Ajinenko et al., Phys.Lett. **B574**(2003), 14.

[5] I.V. Ajinenko et al., Yad.Fiz **65**(2002), 2125.

[6] R Brun et al., CERN-DD/EE/84-1.

[7] J. Gasser, H. Leutwyler Nucl. Phys. **B250**(1985), 517.

[8] H. Steiner et al., Phys.Lett. **B36**(1971), 521.

[9] M.V. Chizhov, Phys.Lett. **B381**(1996), 359.

[10] L. Rosselet et al., Phys.Rev. **D15**(1977), 574.

[11] F. James, M.Roos, CERN D506,1989.

[12] K.Horie et al., Phys.Lett. **B513**(2001), 311.